PAPER

Syntheses, structures and characteristics of four metal–organic coordination polymers based on 5-hydroxyisophthalic acid and N-containing auxiliary ligands†

Liangliang Zhang,[a] Jie Guo,[b] Qingguo Meng,[b] Rongming Wang*[a] and Daofeng Sun*[ab]

Solvothermal reactions of 5-hydroxyisophthalic acid (hip) and different N-containing auxiliary ligands with transition metal salts provided four new metal–organic coordination polymers (MOPs), namely, $\{Zn(hip)(2,2'\text{-bipy})\cdot2H_2O\}_n$ (**1**), $\{[Ni(hip)(4,4'\text{-bipy})(H_2O)]\cdot DMF\cdot2H_2O\}_n$ (**2**), $\{Zn(hip)(tib)\cdot2H_2O\}_n$ (**3**), $\{[Zn_2(hip)_2]\cdot5H_2O\}_n$ (**4**), (2,2'-bipy = 2,2'-bipyridine, 4,4'-bipy = 4,4'-bipyridine, DMF = N,N'-dimethylformamide, tib = 1,3,5-tris(1-imidazolyl)benzene). All of the complexes have been structurally characterized by single-crystal X-ray diffraction analyses, infrared spectra (IR), elemental analyses and powder X-ray diffraction (PXRD). Single crystal X-ray diffraction analysis reveals that complex **1** exhibits a one-dimensional zig-zag chain, in which strong $\pi\cdots\pi$ interactions are found between neighbouring 2,2'-bipy molecules. Complex **2** has a 2D double-layer square framework, exhibiting AA stacking sequence, and the topology of each layer is typical 2D (4^4)-sql. In complex **3**, both hip and tripodal ligand tib act as bidentate bridging ligand and extend the tetragonal pyramid Zn(II) centers to a 2D wavy framework, exhibiting an AB stacking sequence. The 2D layer structures in **2** and **3** are different from each other. In complex **4**, the oxygen atoms of the hydroxy group of hip participate in constructing a framework, which results to the 3D net framework with 1D channel. The structural and topological differences of the four MOPs indicate that the auxiliary ligand play important roles in the formation of final structures. Furthermore, the thermal stability and photoluminescence properties of complexes **1**–**4** were investigated.

Introduction

In recent years, the rational design and synthesis of novel metal organic coordination polymers (MOPs) has become an active topic of investigation, owing to their fascinating structural versatility and their tremendous functional properties in gas storage, chemical separations, ion exchange, microelectronics, nonlinear optics, and catalysis.[1–4] Many coordination polymers with intriguing topologies and properties have been reported,[5] but the control of structural dimensionality remains a great challenge in crystal engineering.[6] Generally, the construction of MOPs is seriously affected by the bewildering structure-directing factors such as the metal ions, the

predesigned organic linkers, solvent, pH value of the solution, the temperature, the counter ion with different bulk or coordination ability, the template and metal-to-ligand stoichiometry, *et al.*[7,8]

Carboxylates are often employed as bridging ligands to construct coordination polymers because of their versatile coordination modes and their ability to act as H-bond acceptors and donors.[9] Our investigations were focused on the 5-hydroxyisophthalic acid (hip) ligand. We chose hip based on the following considerations: (1) compared to many other polycarboxylates, hip has a higher solubility in many organic solutions, which impedes the precipitate; (2) the ligand has two carboxyl groups and one hydroxyl, providing abundant coordination and H-bond sites, which may facilitate the formation of novel topologies and supramolecular assembly.

Apart from the carboxylates linkers, the utilization of auxiliary ligands strategy leading to different structures in the formation of coordination complexes is of enormous importance. A lot of MOPs structures have been demonstrated based on mixed organic ligands.[10] N-containing auxiliary ligands were frequently selected to explore the effect on the coordination modes of ligands, such as 2,2'-bipy, 4,4'-bipy

[a] *College of Science, China University of Petroleum (East China), Qingdao, Shandong 266580, People's Republic of China. E-mail: dfsun@upc.edu.cn*
[b] *Key Lab of Colloid and Interface Chemistry, Ministry of Education, School of Chemistry and Chemical Engineering, Shandong University, Jinan, Shandong, 250199, People's Republic of China*
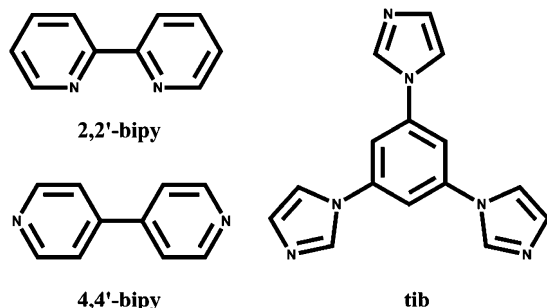
Scheme 1 N-containing ligands involved in this work.

and tib, in which 2,2'-bipy adopts a chelating mode; 4,4'-bipy is the bridging ligand; and tib belongs to the tripodal imidazole ligand (Scheme 1). The particular behavior allows them to be promising candidates for designing beautiful metal building blocks.[11]

As a result, solvothermal reactions of hip and metal ions (Zn and Ni), with the aid of N-containing auxiliary ligands, resulted in the formation of four new metal organic coordination complexes with different dimensions, $\{Zn(hip)(2,2'\text{-bipy})\cdot 2H_2O\}_n$ (**1**), $\{[Ni(hip)(4,4'\text{-bipy})(H_2O)]\cdot DMF\cdot 2H_2O\}_n$ (**2**), $\{Zn(hip)(tib)\cdot 2H_2O\}_n$ (**3**), $\{[Zn_2(hip)_2]\cdot 5H_2O\}_n$ (**4**), (2,2'-bipy = 2,2'-bipyridine, 4,4'-bipy = 4,4'-bipyridine, DMF = N,N'-dimethylformamide, tib = 1,3,5-tris(1-imidazolyl)benzene). Complexes **1**–**4** were characterized by elemental analysis (EA), single-crystal X-ray crystallography, powder X-ray diffraction (PXRD), infrared spectroscopy (IR), and thermogravimetric analyses (TGA), and the luminescent properties of compounds **1**–**4** and hip have also been investigated. Moreover, the coordination modes of the hip ligand as well as the structure comparisons of the complexes are discussed in detail.

Experimental section

Materials and general methods

All chemicals were of reagent grade and were used as commercially obtained without further purification. Elemental analyses (for C, H or N) were carried out on a Perkin-Elmer 240 elemental analyzer. Powder X-ray diffraction measurements were performed with a Bruker AXS D8 Advance instrument. The FT-IR spectra were recorded in the range 4000–400 cm^{-1} on a Nicolet 330 FTIR Spectrometer using the KBr pellet method. Thermogravimetric analysis (TGA) experiments were performed using a Perkin-Elmer TGA 7 instrument (heating rate of 10 °C min^{-1}; nitrogen stream). Photoluminescence spectra were measured on an F-280 fluorescence spectrophotometer.

Preparation of complexes 1–4

$\{Zn(hip)(2,2'\text{-bipy})\cdot 2H_2O\}_n$ (**1**). A mixture of hip (10 mg, 0.05 mmol), $Zn(NO_3)_2\cdot 6H_2O$ (29.7 mg, 0.1 mmol) and 2,2'-bipy (15.6 mg, 0.1 mmol) were dissolved in 1.5 mL of mixed solvents of DMF, EtOH and H_2O (v/v/v = 5 : 2 : 1). After ultrasonication at room temperature for 10 min, the glass tube was sealed and placed in an oven and slowly heated to

110 °C from room temperature over 10 h, kept at 110 °C for 50 h, and then slowly cooled to 30 °C in 800 min. The colorless crystals were collected and dried in air. (Yield: 60%, based on zinc.) Anal. calc. (found) for $C_{18}H_{12}N_2O_5Zn$: C, 54.00 (53.37); H, 3.02 (3.20); N, 6.97 (6.46) %. IR (KBr): $v(cm^{-1})$ = 3507 (s), 3179 (m), 3078 (w), 2929 (w), 1664 (s), 1381 (s), 1274 (s), 1097 (s), 789 (s), 718 (s), 655 (m).

$\{[Ni(hip)(4,4'\text{-bipy})(H_2O)]\cdot DMF\cdot 2H_2O\}_n$ (**2**). A mixture of hip (10 mg, 0.05 mmol), $Ni(NO_3)_2\cdot 6H_2O$ (29.0 mg, 0.1 mmol) and 4,4'-bipy (15.6 mg, 0.1 mol) was dissolved in 1.5 mL of mixed solvents of DMF, EtOH and H_2O (v/v/v = 1 : 1 : 1). After ultrasonication at room temperature for 10 min, the glass tube was sealed and placed in an oven and slowly heated to 115 °C from room temperature in 10 h, kept at 115 °C for 50 h, and then slowly cooled to 30 °C in 800 min. The green crystals were collected and dried in air. (Yield: 37%, based on nickel.) Anal. calc. (found) for $C_{18}H_{10}N_2O_7Ni$: C, 50.87 (51.27); H, 2.37 (2.85); N, 6.59 (6.07) %. IR (KBr): $v(cm^{-1})$ = 3563 (s), 3489 (s), 3184 (m), 3074 (m), 1968 (w), 1599 (s), 1380 (s), 1279 (s), 1218 (s), 829 (s), 780 (s), 726 (s), 637 (s), 487 (m).

$\{Zn(hip)(tib)\cdot 2H_2O\}_n$ (**3**). A mixture of hip (10 mg, 0.05 mmol), $Zn(NO_3)_2\cdot 6H_2O$ (29.7 mg, 0.1 mmol) and tib (17 mg, 0.06 mmol) were dissolved in 1.5 mL of mixed solvents of DMF, H_2O (v/v = 2 : 1) and one drop of KOH (0.1 mol dm^{-3}) solution. After ultrasonication at room temperature for 10 min, the glass tube was sealed and placed in an oven and slowly heated to 120 °C from room temperature in 10 h, kept at 120 °C for 66 h, and then slowly cooled to 30 °C in 800 min. The colorless crystals were collected and dried in air. (Yield: 63%, based on zinc.) Anal. calc. (found) for $C_{23}H_{17}N_6O_5Zn$: C, 52.84 (52.64); H, 3.28 (3.49); N, 16.07 (16.37) %. IR (KBr): $v(cm^{-1})$ = 3444 (s), 3150 (m), 3105 (m), 2959 (w), 2836 (w), 1628 (s), 1566 (s), 1503 (m), 1343 (m), 1243 (w), 1067 (w), 784 (w), 727 (w), 648 (w).

$\{[Zn_2(hip)_2]\cdot 5H_2O\}_n$ (**4**). A mixture of hip (10 mg, 0.05 mmol), $Zn(NO_3)_2\cdot 6H_2O$ (29.7 mg, 0.1 mmol) were dissolved in 1.5 mL of mixed solvents of DMF, EtOH (v/v = 1 : 1). After ultrasonication at room temperature for 10 min, the glass tube was sealed and placed in an oven and slowly heated to 110 °C from room temperature in 10 h, kept at 110 °C for 50 h, and then slowly cooled to 30 °C in 800 min. The colorless crystals were collected and dried in air. (Yield: 25%, based on zinc.) Anal. calc. (found) for $C_{16}H_6NO_{10}Zn_2$: C, 38.21 (37.94); H, 1.20 (1.23); N, 2.78 (2.56) %. IR (KBr): $v(cm^{-1})$ = 3452 (w), 3195 (w), 2970 (w), 2783 (w), 1656 (s), 1580 (s), 1371 (s), 1278 (s), 1209 (m), 1101 (m), 1007 (m), 887 (w), 800 (m), 778 (s), 730 (s), 658 (w), 472 (m).

X-ray crystallography

Single crystals of compounds **1**–**4** with appropriate dimensions were chosen under an optical microscope and quickly coated with high vacuum grease (Dow Corning Corporation) before being mounted on a glass fiber for data collection. Data were collected on a Bruker Apex II Image Plate single-crystal diffractometer with graphite-monochromated Mo Kα

Table 1 Crystal data for **1–4**

Compound	1	2	3	4
Formula	$C_{18}H_{12}N_2O_5Zn$	$C_{18}H_{10}N_2O_7Ni$	$C_{23}H_{17}N_6O_5Zn$	$C_{16}H_6NO_{10}Zn_2$
M_r	401.67	424.99	522.80	504.95
Crystal system	Monoclinic	Triclinic	Monoclinic	Monoclinic
Space group	$C2/c$	$P\bar{1}$	$P2_1/c$	$P2_1/c$
a (Å)	13.629(3)	10.163(6)	9.6938(14)	16.784(2)
b (Å)	24.248(5)	10.737(6)	13.682(2)	12.9256(18)
c (Å)	14.286(3)	11.300(6)	16.569(2)	14.555(2)
α (°)	90.00	74.521(9)	90.00	90.00
β (°)	104.645(3)	89.840(9)	93.601(2)	108.565(2)
γ (°)	90.00	68.492(9)	90.00	90.00
Z	8	2	4	4
V (Å^3)	4567.8(17)	1099.3(11)	2193.3(6)	2993.3(7)
D_c (g cm^{-3})	1.168	1.284	1.583	1.120
μ (mm^{-1})	1.099	0.919	1.170	1.639
$F(000)$	1632.0	432.0	1068.0	1000.0
No. of unique reflns	11 113	5354	10 718	14 402
No. of obsd reflns [$I > 2\sigma(I)$]	4009	3780	3860	5251
Parameters	235	279	316	262
GOOF	0.961	1.057	1.026	1.054
Final R indices [$I > 2\sigma(I)$]^{a,b}	$R_1 = 0.0447$, w$R_2 = 0.1201$	$R_1 = 0.0547$, w$R_2 = 0.1613$	$R_1 = 0.0364$, w$R_2 = 0.0875$	$R_1 = 0.0695$, w$R_2 = 0.2229$
R indices (all data)	$R_1 = 0.0623$, w$R_2 = 0.1278$	$R_1 = 0.0618$, w$R_2 = 0.1670$	$R_1 = 0.0539$, w$R_2 = 0.0962$	$R_1 = 0.0768$, w$R_2 = 0.2315$

^{a} $R_1 = \Sigma||F_o| - |F_c||/\Sigma|F_o|$. ^{b} w$R_2 = [\Sigma w(F_o{}^2 - F_c{}^2)^2/\Sigma w(F_o{}^2)^2]^{0.5}$.

radiation source (λ = 0.71073 Å) operating at 50 kV and 30 mA for **1–4**. All absorption corrections were applied using the multiscan program SADABS.[12] In all cases, the highest possible space group was chosen. All structures were solved by direct methods using SHELXS-97[13] and refined on F^2 by full-matrix least-squares procedures with SHELXL-97.[14] Atoms were located from iterative examination of difference F-maps following least squares refinements of the earlier models. Hydrogen atoms were placed in calculated positions and included as riding atoms with isotropic displacement parameters 1.2 times U_{eq} of the attached C atoms. All structures were examined using the Addsym subroutine of PLATON[15] to assure that no additional symmetry could be applied to the models. The crystallographic details of **1–4** are summarized in Table 1. Selected bond lengths and angles for **1–4** are collected in Table S1, ESI.† The hydrogen bond geometries for **1–4** are shown in Table S2 (ESI†).

Results and discussion

Synthesis

Crystallization of all complexes **1–4** were obtained under similar reaction conditions by the solvothermal method, which has been proven to be an effective and powerful in the self-assembly of metal–organic coordination polymers. By changing the auxiliary ligand, compounds **1–3** and **4** have been synthesized.

Descriptions of the crystal structures

{Zn(hip)(2,2'-bipy)·2H$_2$O}$_n$ (1). X-ray crystallographic analysis reveals that **1** bears a one-dimensional zig-zag chain, crystallizing in monoclinic $C2/c$ space group. There is one Zn(II) ion, one hip ligand and one 2,2'-bipy in the asymmetric unit. As shown in Fig. 1a, the five-coordinated Zn(II) adopts a distorted [ZnN$_3$O$_2$] square pyramid geometry, where three O atoms from the carboxylic group (O1, O2, O3) of three hip ligands, and two N atoms (N1, N2) are from one 2,2'-bipy molecule. The Zn–O distances range from 2.1551(14) to 2.2198(14) Å, and the distance of Zn–N is 2.1867(15) Å. In compound **1**, two carboxylic groups of the hip ligand adopt μ_1-η^1-η^0 and μ_2-η^1-η^1 bridging fashion. Hence, the structure of compound **1** shows that two adjacent and coplanar hip molecules link four Zn(II) atoms to form a 16-membered-ring, and then 16-membered-rings connect each other to furnish a one-dimensional zig-zag chain by [Zn$_2$(CO$_2$)$_2$] units with the distance of neighbouring Zn ions being 4.64(7) Å. A pair of bipy molecules occupy the left coordination sites, which interrupt to construct high-dimensional architectures (Fig. 1b).

As depicted in Fig. 1c, the most fascinating feature of **1** is the large dumbbell-like channels composed by $\pi\cdots\pi$ interactions, which is observed between two adjacent bipy molecules from one and the same zig-zag chain or two neighboring zig-zag chain, with centroid-to-centroid distances of 3.635(7) and 3.877(4) Å. O–H$\cdots$O hydrogen bond interactions are also found between the hydroxy group of hip and the carboxylate oxygen atoms together with weak C–H$\cdots$O hydrogen bond interactions. The significant $\pi\cdots\pi$ and hydrogen bond interactions are thought to play a key role for the stability of the crystal lattice. Therefore, the structure of **1** forms a final 3D supramolecular framework with large dumbbell-like channels, which occupy a 23.2% solvent-accessible volume calculated from PLATON as shown in Fig. 1d. [Symmetry code: (a) $-x$, y, 0.5 $- z$; (b) 0.5 $- x$, 0.5 $- y$, 1 $- z$.]

Previously, Plater *et al.* employed zinc acetate, 5-hydroxyisophthalic acid and 2,2'-bipy to obtain a 1D chain coordination polymer with the formula of [Zn(C$_8$H$_4$O$_5$)(2,2'-bipy)]$_n$, which was connected by a Zn$_2$C$_2$O$_4$
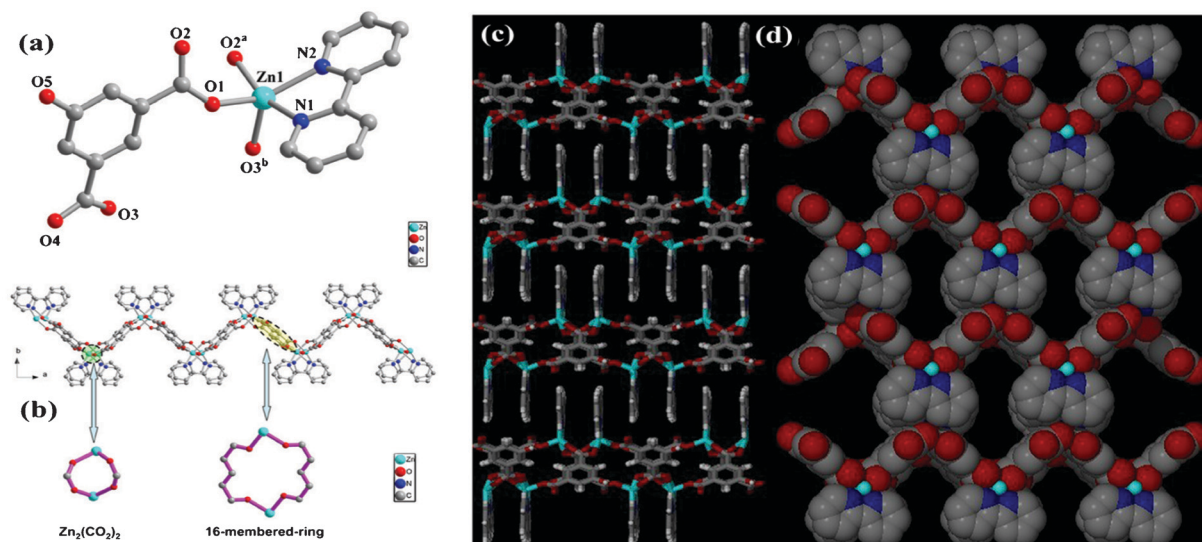
Fig. 1 (a) The coordination environment of the Zn(II) ion in **1**. [Symmetry code: (a) −x, y, 0.5 − z; (b) 0.5 − x, 0.5 − y, 1 − z.] (b) 1D zig-zag chain formed by [Zn₂(CO₂)₂] units and 16-membered-ring viewed from c direction. (c) Ball-and-stick packing of **1** viewed from a direction. (d) Space-filling of **1** viewed from c direction. All H atoms are omitted for clarity.

ring and 5-hydroxyisophthalic acid ligand;[16] Yin *et al.* used $Zn(NO_3)_2 \cdot 6H_2O$ with the same mixed ligands to assemble a 1D ribbon with the formula of $\{[Zn(C_8H_4O_5)(C_{10}H_8N_2)]\cdot H_2O\}_n$, which was constructed by ZnN_2O_4 and 5-hydroxyisophthalic acid ligand.[17] Based on the structural analysis, complex **1** in our work is different from the above two coordination polymers. Comparing the results indicates that the reagent ratios, solvent, temperature or reaction vessel may strongly influence the resulting structures, which also suggests that the design and prediction of coordination polymer structures are still very difficult, even if the same reagents are used.

$\{[Ni(hip)(4,4'-bipy)(H_2O)]\cdot DMF\cdot 2H_2O\}_n$ (**2**). X-ray single crystal diffraction exhibits that complex **2** has a 2D double-layer square framework and crystallizes in triclinic $P\bar{1}$ space group. The asymmetrical unit contains one Ni(II) ion, one hip ligand, one disordered 4,4'-bipy, and one coordination and one lattice water molecule. The coordination environment of the Ni(II) ion is shown in Fig. 2a. Ni(II) is coordinated to three carboxylate oxygen atoms from two hip ligands, one oxygen atom from the coordinated water molecule, and two nitrogen atoms from two 4,4'-bipy in the axial direction, forming an enlarged octahedron geometry. The Ni–O distances ranged from 2.024(3) Å to 2.179(3) Å, the distance of Ni–Ow is 2.055(3) Å, and Ni–N distances range from 2.100(3) to 2.132(3) Å. The mean Ni–O and Ni–N bond lengths (2.101(8) Å and 2.116(3) Å) are comparable to those of the reported similar complexes.[18] The carboxylate group in compound **2** adopts μ_1-η^1-η^1 and μ_2-η^1-η^1 bridging modes to link two Ni(II) ions along one direction to form a hip–Ni–hip chain, and then the linear 2,2'-bipy ligand links these chains in a vertical direction, which results in the final 2D square structure (extending along the ac plane) (Fig. 2b).

The topological analysis of one layer in complex **2** has also been performed. It has a typical 2D (4^4)-sql layer framework,

and the length of squares is 10.16 (distance of neighbour Ni separated by hip ligand) and 11.30 Å (distance of neighbour Ni separated by 4,4'-bipy ligand). As illustrated in Fig. 2c and 2d, complex **2** exhibits AA stacking double-layered framework along the plane ac, which involves O–H⋯O and C–H⋯O hydrogen bond interactions among the hydroxy group, lattice and coordination water molecules, and carboxylate oxygen atoms of hip. These interactions not only consolidate the 2D structures but also make the 3D supramolecular structures form finally. [Symmetry code: (a) 1 + x, y, z).]

$\{Zn(hip)(tib)\cdot 2H_2O\}_n$ (**3**). When we used a tripodal imidazole ligand (tib) instead of rigid 4,4'-bipy or 2,2'-bipy, complex **3** was obtained in a good yield. X-ray single crystal diffraction indicates that complex **3** has a 2D wavy framework and crystallizes in monoclinic $P2_1/c$ space group. The asymmetric unit contains one Zn(II) ion, one hip ligand, and one tib molecule. The coordination environment of Zn(II) ion is shown in Fig. 3a. It is coordinated to three carboxylate oxygen atoms from two hip ligands and two nitrogen atoms from two tib molecules, forming tetragonal pyramid geometry. The Zn–O and Zn–N distances range from 1.929(2) to 1.948(2) Å and 2.022(3) to 2.027(3) Å, respectively. In compound **3**, all carboxylate groups adopt μ_1-η^1-η^0 bridging mode to link two Zn(II) ions along one direction to form a hip–Zn–hip chain, and then linear tib ligands link these chains in a vertical direction, which results in the final 2D wavy structure (Fig. 3b). Only two of the imidazole nitrogen atoms of the tib molecule participate in the construction of the 2D wavy structure. Hence, the tib can also be thought of as a two-connected ligand. At the same time, because of the synergistic effect of electronic and steric hindrance effect between the imidazole ring and the central benzene ring, the coordination mode of tib is not strictly linear, which satisfies the tetragonal pyramid
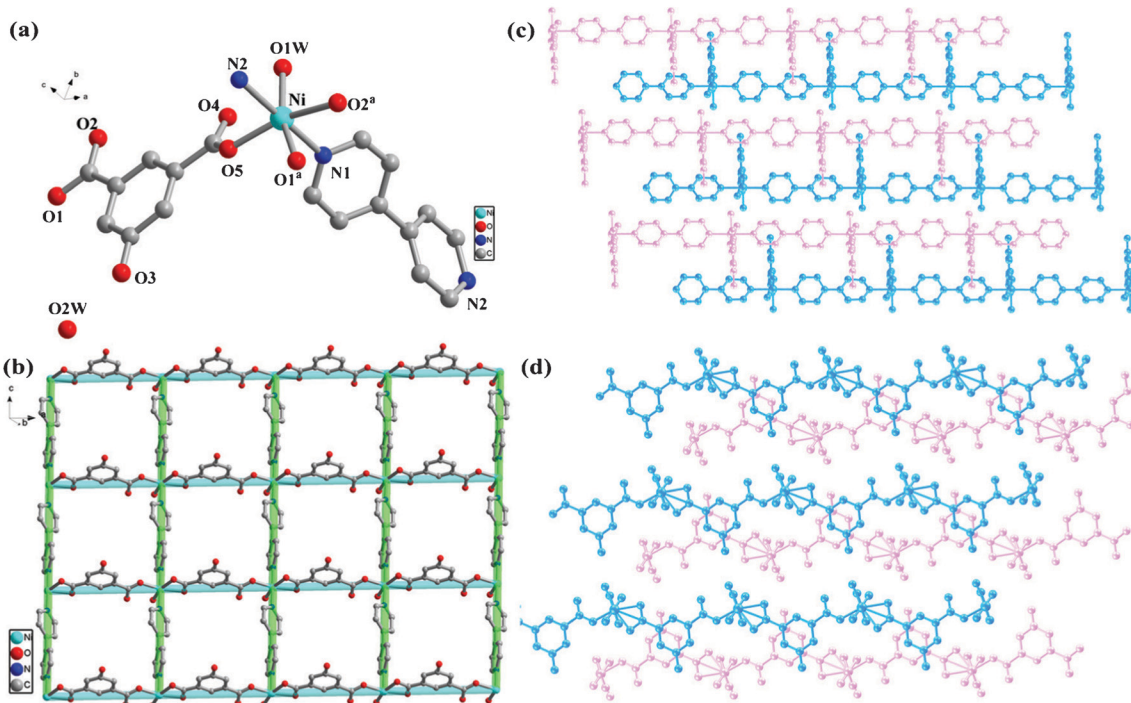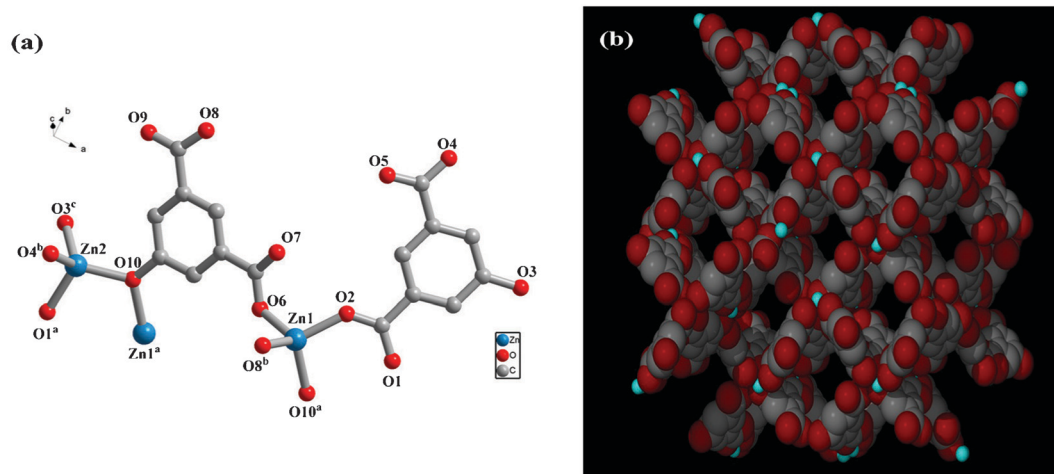
Fig. 2 (a) The coordination environment of the Ni(II) ion in **2**. [Symmetry code: (a) 1 + *x*, *y*, *z*).] (b) Single-layer 2D square structure in **2** constructed by two-connected hip and 4,4'-bipyridyl ligands. (c) The double-layer structure of **2** viewed along the *a* direction. (d) The double-layer structure of **2** viewed along the *c* direction. Hydrogen atoms are omitted for clarity.

coordination geometry of Zn(II) ion. It should be mentioned that there are two kinds of Zn–Zn distances: one (9.6938(14) Å) is connected by the hip molecule, the other (12.9303(14) Å) is linked by the tib ligand, which is a little longer than that in compound **2**.

The topological analysis of complex **3** has also been performed. Compared with complex **2**, complex **3** also has a 2D (4^4)-sql layer topology by considering Zn ions as nodes, and tib and hip as 2-connected linkers. However, their 2D layer structure (2D square in **2** *vs.* 2D wavy in **3**) have an
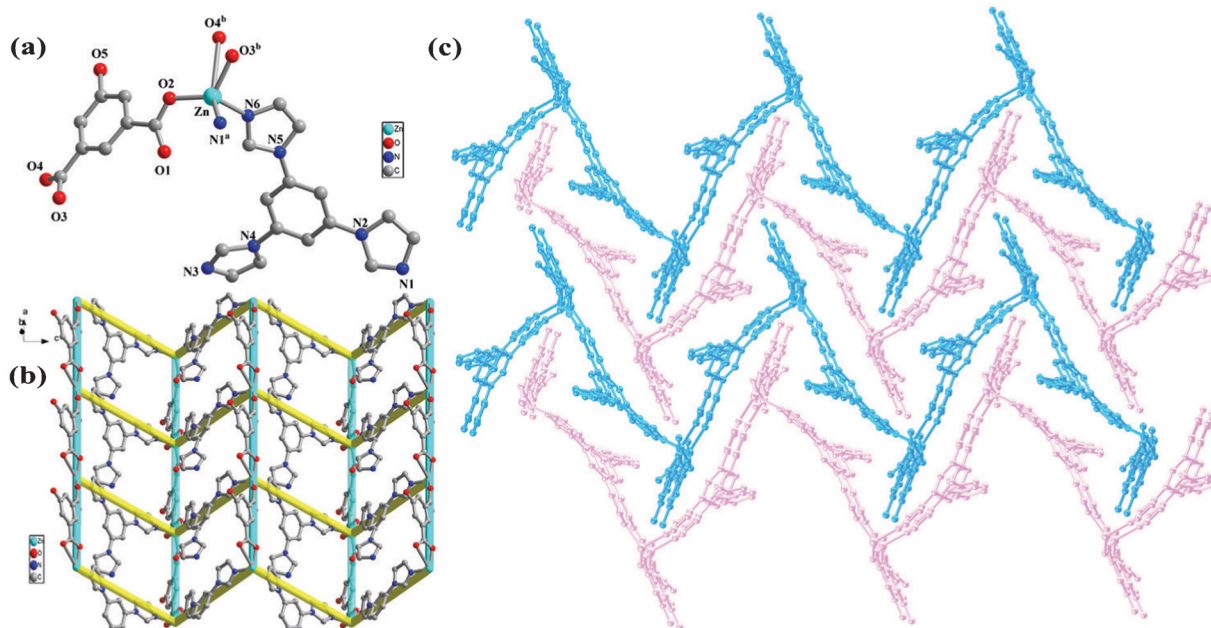
Fig. 3 (a) The coordination environment of the Zn(II) ion in **3**. Hydrogen atoms are omitted for clarity. [Symmetry code: (a) *x*, 0.5 − *y*, 0.5 + *z*; (b) 1 + *x*, *y*, *z*.] (b) 2D wavy structure constructed by two-connected hip and tib ligands. (c) 3D supramolecular structure of **3**.

(a)

(b)

Fig. 4 (a) The coordination environment of the Zn(II) ion in **4**. Hydrogen atoms are omitted for clarity. [Symmetry code: (a) −x, 1 − y, −z; (b) −x, −0.5 + y, 0.5 − z; (c) −1 + x, 1.5 − y, −0.5 + z.] (b) 3D frameworks of **4** with a 1D channel.

obvious difference since the length and angle of tib and 4,4'-bipy ligands are different. (Fig. 3c). [Symmetry code: (a) x, 0.5 − y, 0.5 + z; (b) 1 + x, y, z.]

$\{[Zn_2(hip)_2]\cdot 5H_2O\}_n$ (**4**). X-ray single crystal diffraction indicates that complex **4** has a 3D net framework and crystallizes in monoclinic $P2_1/c$ space group. The asymmetrical unit contains two Zn(II) ions, two hip and one lattice water molecule. The coordination environment of Zn(II) ion is shown in Fig. 4a. Both Zn1 and Zn2 are coordinated to three carboxylate oxygen atoms from three hip ligands, one oxygen atom from the phenolic hydroxyl group of one hip molecule, forming a tetrahedron geometry. Meanwhile, Zn1 and Zn2 were connected by oxygen atoms to furnish a dinuclear $[Zn_2O_8]$ SBUs. The Zn–O distances range from 1.931(5) to 1.995(4) Å, which are in the normal ranges.[19] The carboxylate groups in compound **4** adopts μ_1-η^1-η^0 and μ_2-η^1-η^1 bridging mode to link four Zn(II) ions, which results in the final 3D square structure. The structure shows small 1D channels with a window size of 8.08 × 9.61 Å^2 along a axis, in which the disordered solvent molecules reside (Fig. 4b). The solvent accessible volume is estimated by using the PLATON program to be about 27.4% of the total crystal volume.

Xiao *et al.* used $Zn(NO_3)_2\cdot 6H_2O$ and 5-hydroxyisophthalic acid to synthesize a zig-zag chain under the conditions of the liquid diffusion method, in which the hip ligand adopts a μ_2-η^1-η^1 bridging mode.[20] The structural differences between this complex and compound **4** further indicated that the construction of MOPs was seriously affected by the bewildering structure-directing factors.

Comparison of the crystal structures

Single-crystal X-ray diffraction analyses reveal that complexes **1**–**4** exhibit structural diversity from 1D chains, 2D layers to 3D net frameworks. From the structural point of view, the different structures maybe partly attributed to the versatile coordination modes of hip anions, which are listed in Scheme 2.

In complex **1**, hip adopts mode A to connect three five-connected zinc ions, forming the one-dimensional zig-zag chain. Mode B appears in **2**, the 2D layer square framework is formed by linking hip to two six-connected nickel ions, which connect with two-connected 4,4'-bipyridyl. Mode C is observed in **3**, hip joins two four-connected zinc ions, together with two-connected tib, which leads to a 2D wavy framework. In complex **4**, the mode D is adopted, and the 3D net framework is obtained since the oxygen atoms of the hydroxy group of hip participate in the coordination.

Effects of N-connecting ligand and solvent system on the structure

The design and synthesis of novel structure and specific functionality MOPs has been a goal, constantly pursued in the
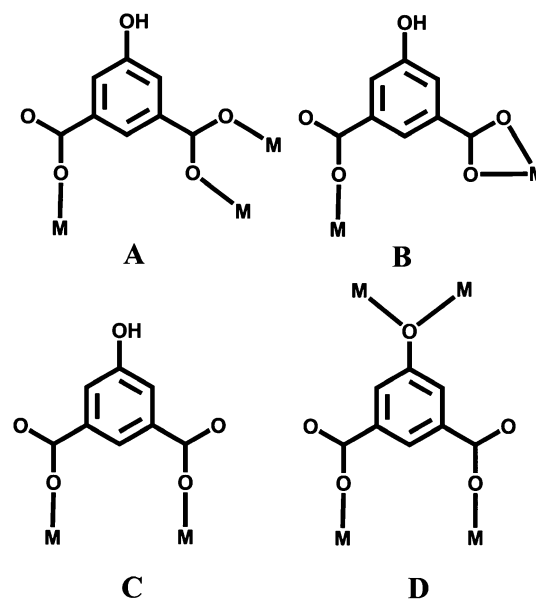
Scheme 2 Coordination mode of hip in **1**–**4**.

field of coordination chemistry. The key strategy rests on the selection of organic ligands bearing various geometry, length and flexibility, another important factor is the using of an auxiliary ligand. In the present work, we selected different N-connecting ligands. For example, 2,2'-bipyridyl acts as a chelating ligand, 4,4'-bipyridyl is a two-connected ligand, and tib has a tripodal configuration and coordination possibilities. But in complex **3**, all imidazole groups of each tib ligand coordinate through only two nitrogen atoms, leaving one uncoordinated nitrogen atom. Comparing **2** with **3**, though both **2** and **3** are 2D layer structures, the differences of auxiliary ligand in terms of lengths and angles may play a vital role in the final structure (2D double-layer square *vs.* 2D wavy layer).

Moreover, the structures of complexes **1–4** are also influenced by the solvent systems. The dimensionality and topology of networks are mainly determined by the coordination modes of hip and the N-connecting ligand, which are clearly dominated but involve the effect by of the solvent molecules to some extent. For complexes **1** and **2**, both of them were obtained in DMF–C_2H_5OH–H_2O, but the proportions of ingredient solvents are different (5 : 2 : 1 *vs.* 1 : 1 : 1). In **2**, the water molecule occupies one of the coordination sites of nickel, which interrupts to construct high-dimensional architectures. Meanwhile, one lattice water molecule is found in

its asymmetrical unit of **2**, acting as both donor and acceptor of hydrogen bonds. Plater and Yin *et al.* used water as a solvent and the same mixed ligands to assemble two similar coordination complexes with the formulae of $[Zn(C_8H_4O_5)(2,2'\text{-bipy})]_n$ and $\{[Zn(C_8H_4O_5)(C_{10}H_8N_2)]\cdot H_2O\}_n$, respectively.[16,17] The differences in dimensionality and structure may contribute to the solubility of hip and N-connecting ligand in water or DMF–C_2H_5OH–H_2O. For **3**, 1.5 mL of mixed solvents of DMF and H_2O (v/v = 2 : 1) were used with the addition of one drop KOH (0.1 mol L^{-1}) solution, which makes tib ligands partially deprotonated. Therefore, one non-coordination nitrogen atom is left and then makes tripodal tib become a two-connected ligand. However, the oxygen atoms of hydroxy group hip participate in construction of the framework in complex **4**, which is obtained in mixed solvents of DMF and EtOH (v/v = 1 : 1). The results indicate that the solvent systems have a remarkable effect on the formation of MOP structures.

IR spectra, X-ray powder diffraction analyses and thermal analyses

The IR spectra of compounds **1–4** show the sharp bands in the ranges of 1700–1600 and 1400–1300 cm^{-1}, which are attributed to asymmetric and symmetric stretching vibrations
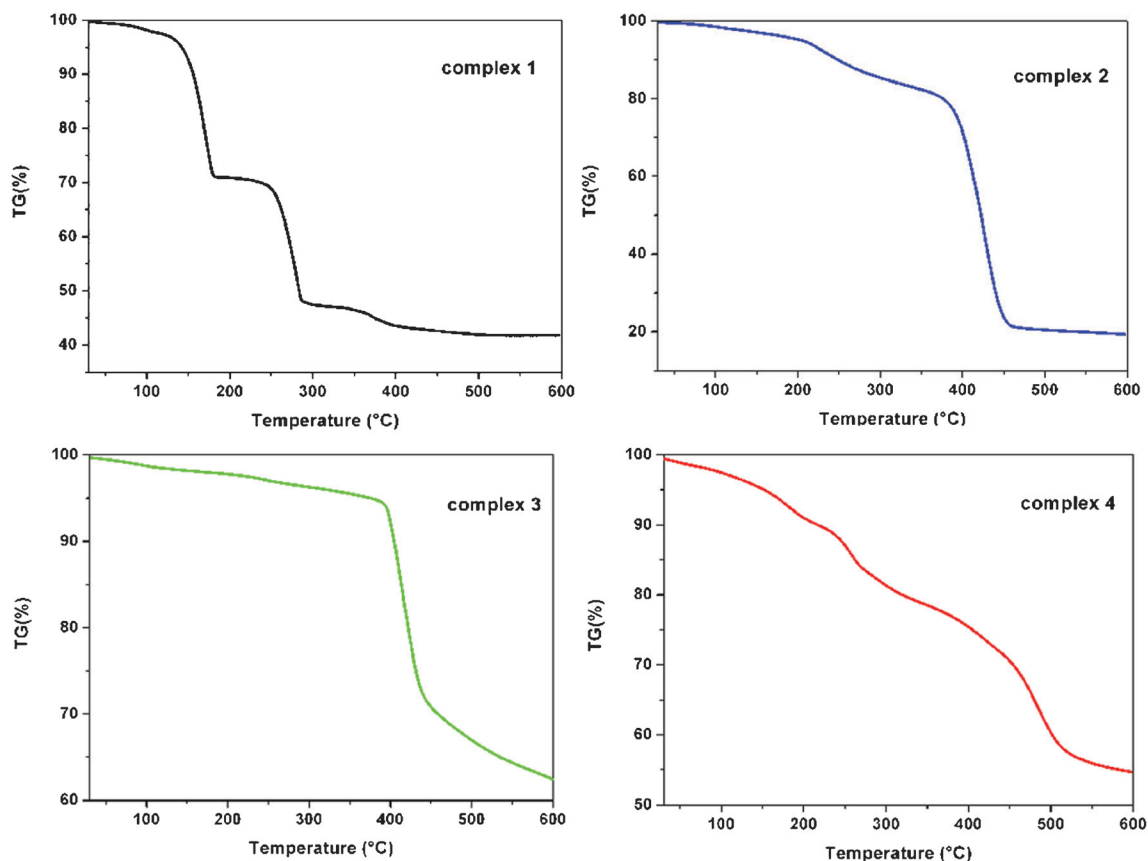

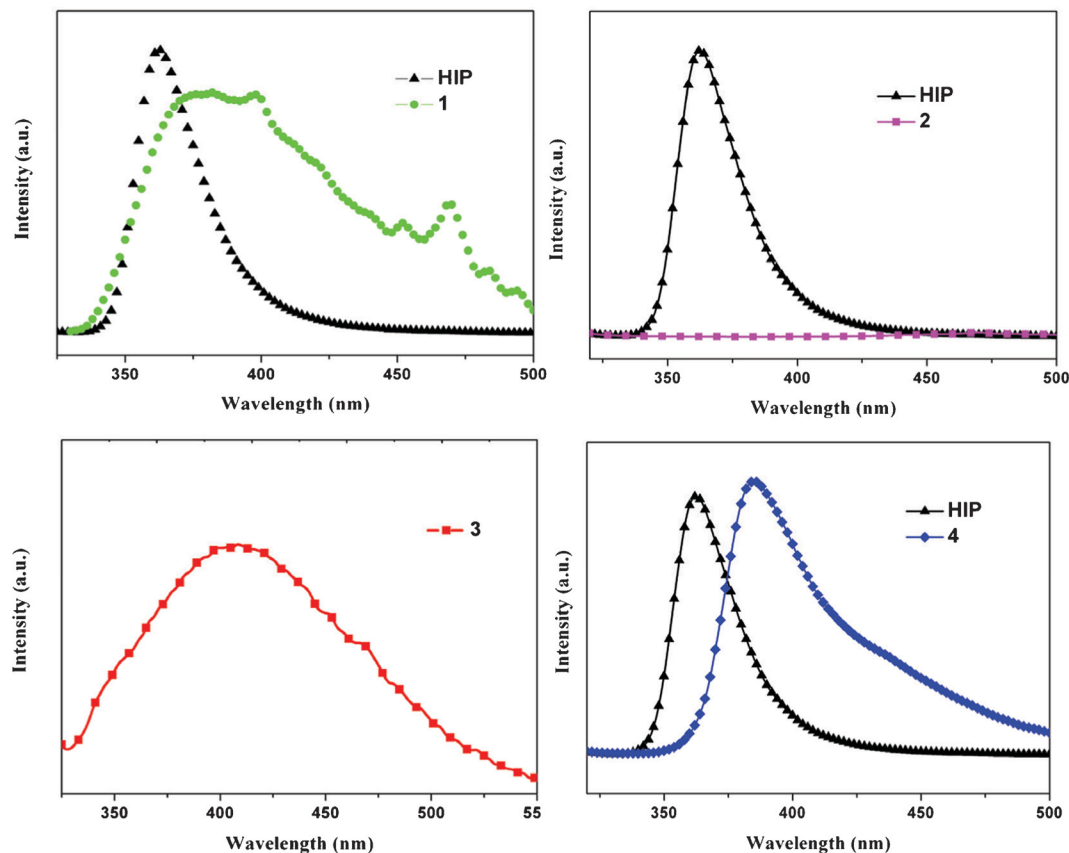**Fig. 5** TGA curves for complexes **1–4**.

Fig. 6 Photoluminescence of the free ligand and complexes **1–4**.

of the carboxylic group, respectively.[21] To confirm the phase purity of complexes **1–4**, the PXRD patterns were also recorded at room temperature. As shown in Fig. S1 (ESI†), all the PXRD patterns measured for the as-synthesized samples are in good agreement with the PXRD patterns simulated from the respective single-crystal X-ray data using the Mercury 3.1 program, demonstrating the phase purity of the products. The dissimilarities in intensity may be due to the preferred orientation of the crystalline powder samples.

To assess the thermal stability and their structural variation with the temperature, thermogravimetric analysis (TGA) of compounds **1–4** was performed under a N_2 atmosphere by using single-phase polycrystalline samples (Fig. 5). Complex **1** has two identifiable weight loss steps: the first one is consistent with the removal of lattice water and 2,2'-bipy molecule (obsd 43.7%, calcd 44.6%), which appears between 100 and 184 °C. The second one is attributed to the collapse of the framework, which is in the range of 184 to 290 °C. For **2**, the first weight loss from 249 °C is consistent with the removal of lattice and coordinated water, and DMF molecule (obsd 24.2%, calcd 22.3%). The second one from 249 to 375 °C is assigned to the collapse of the framework. Complex **3** continuously loses lattice solvent molecules before 390 °C, and then the framework of **3** collapsed after this temperature. Complex **4** has a successive weight loss

process, indicating the instability of frameworks during heating.

Photoluminescence properties

Based on the various applications in chemical sensors, photochemistry and electroluminescent display, the luminescent coordination compounds are of great current interest to chemical researchers.[22] Although still in its early stages, the unique characteristics of these MOPs materials provide a platform for understanding light emission with both unparalleled synthetic flexibility and a highly ordered, inherently quantifiable, structure. From a practical point of view, it is also becoming clear that luminescence spectroscopy is a superb tool for assessing the structural integrity and purity of MOPs, with sensitivity far exceeding that of powder X-ray diffraction (PXRD). The photoluminescence spectra of complexes **1–4**, tib and hip were investigated in the solid state at room temperature, as shown in Fig. 6. Upon the irradiation of ultraviolet light at 300 nm, the free ligand hip displays a strong emission with a maxima at 362 nm, which can be attributed to the intraligand $\pi^* \rightarrow \pi$ transition. The free ligand tib shows an emission with a maxima at 397 nm, which is assigned to the $\pi^* \rightarrow \pi$ transition of tib as previously reported.[23] Complex **1** exhibits a broad emission with a maximum at 381 nm, which is attributed to the emission of the

hip ligand. Complex **2** displays almost no luminescent emission in comparison with the free ligand. The emission of this compound becomes drastically quenched, probably owing to d–d electron transitions and vibrations of single electrons, such as Co(II) and Ni(II). The maximum of complex **3** is located at 405 nm, which belongs to the emission of tib. The emission peak of complex **4** appears at 385 nm with 25 nm of red shift when compared with the hip ligand, which is probably assigned to a mixture characteristic of intraligand and ligand-to-ligand charge transition (LLCT) as Zn(II) ion belongs to d^{10} electronic configurations and is difficult to oxidize or reduce.[24] At the same time, the increase of intensity is probably due to the rigidity of ligands which is restricted to the periodic coordinated structure, with the decrease of radiationless decay process of the intraligand ($\pi \rightarrow \pi^*$) excited state and reduced energy loss between intramolecular or intermolecular interactions of organic linkers.[25]

Conclusions

In summary, four metal–organic coordination complexes based on 5-hydroxyisophthalic acid (hip) and different N-containing auxiliary ligands were synthesized and characterized. These complexes show diverse structures and dimensionality from 1D chain (**1**), 2D (4^4)-sql double-layer (**2**), 2D wavy framework (**3**) to 3D net (**4**). The diversity of structures results from different arrangements and coordination fashions of the hip ligand and the various N-containing ligands with different geometries, coordinative abilities and sizes which induce the different coordination spheres of central metal ions. Work is also underway to study more MOPs with fascinating structures and interesting potential properties based on the N-containing ligands materials.

Acknowledgements

Notes and references

1. (*a*) J. L. C. Rowsell and O. M. Yaghi, *Angew. Chem., Int. Ed.*, 2005, **44**, 4670; (*b*) J. P. Zhang, Y. B. Zhang, J. B. Lin and X. M. Chen, *Chem. Rev.*, 2012, **112**, 1001; (*c*) M. K. Kim, C. S. Lim, J. T. Hong, J. H. Han, H. Y. Jang, H. M. Kim and B. R. Cho, *Angew. Chem., Int. Ed.*, 2010, **49**, 364; (*d*) H.-C. Zhou, J. Long and O. M. Yaghi, *Chem. Rev.*, 2012, **112**, 673.

2. (*a*) J. A. Real, E. Andre, M. C. Munoz, M. Julve, T. Granier, A. Bousseksou and F. Varret, *Science*, 1995, **268**, 265; (*b*) S. Leininger, B. Olenyuk and P. J. Stang, *Chem. Rev.*, 2000, **100**, 853; (*c*) O. M. Yaghi, M. O'Keeffe, N. W. Ockwig, H. K. Chae, M. Eddaoudi and J. Kim, *Nature*, 2003, **423**, 705; (*d*) G. Férey and C. Serre, *Chem. Soc. Rev.*, 2009, **38**, 1380; (*e*) M. O'Keeffe and O. M. Yaghi, *Chem. Rev.*, 2012, **112**, 675.

3. (*a*) R. Kitaura, S. Kitagawa, Y. Kubota, T. C. Kobayashi, K. Kindo, Y. Mita, A. Matsuo, M. Kobayashi, H. C. Chang, T. C. Ozawa, M. Suzuki, M. Sakata and M. Takata, *Science*, 2002, **298**, 2358; (*b*) C. Janiak, *Dalton Trans.*, 2003, 2781; (*c*) S. Qiu and G. Zhu, *Coord. Chem. Rev.*, 2009, **253**, 2891; (*d*) H. Kim, G. Park and K. Kim, *CrystEngComm*, 2008, **10**, 954.

4. (*a*) D. Q. Yuan, D. Zhao, D. F. Sun and H. C. Zhou, *Angew. Chem., Int. Ed.*, 2010, **49**, 5357; (*b*) D. F. Sun, S. Q. Ma, Y. X. Ke, D. J. Collins and H. C. Zhou, *J. Am. Chem. Soc.*, 2006, **128**, 3896; (*c*) P. J. Steel, *Acc. Chem. Res.*, 2005, **38**, 243; (*d*) M. H. Zeng, Q. X. Wang, Y. X. Tan, S. Hu, H. X. Zhao, L. S. Long and M. Kurmoo, *J. Am. Chem. Soc.*, 2010, **132**, 2561; (*e*) D. Zhao, D. J. Timmons, D. Yuan and H.-C. Zhou, *Acc. Chem. Res.*, 2011, **44**, 123.

5. (*a*) P. Q. Zheng, Y. P. Ren, L.-S. Long, R.-B. Huang and L.-S. Zheng, *Inorg. Chem.*, 2005, **44**, 1190; (*b*) X.-L. Wang, C. Qin, E.-B. Wang, Y.-G. Li, Z.-M. Su, L. Xu and L. Carlucci, *Angew. Chem., Int. Ed.*, 2005, **44**, 5824; (*c*) P.-X. Yin, J. Zhang, Z.-J. Li, Y.-Y. Qin, J.-K. Cheng, L. Zhang, Q.-P. Lin and Y.-G. Yao, *Cryst. Growth Des.*, 2009, **9**, 4884.

6. (*a*) B. Moulton and M. J. Zaworotko, *Chem. Rev.*, 2001, **101**, 1629; (*b*) A. Bétard and R. A. Fischer, *Chem. Rev.*, 2012, **112**, 1055; (*c*) W. L. Leong and J. J. Vittal, *Chem. Rev.*, 2011, **111**, 688.

7. (*a*) B. K. Roland, C. Carter and Z. P. Zheng, *J. Am. Chem. Soc.*, 2002, **124**, 6234; (*b*) D. Sun, Z. H. Wei, C. F. Yang, D. F. Wang, N. Zhang, R. B. Huang and L. S. Zheng, *CrystEngComm*, 2011, **13**, 1591; (*c*) J. Yang, J. F. Ma, Y. Y. Liu, J. C. Ma and S. R. Batten, *Inorg. Chem.*, 2007, **46**, 6542; (*d*) D. Sun, Y.-H. Li, H.-J. Hao, F.-J. Liu, Y. Zhao, R.-B. Huang and L.-S. Zheng, *CrystEngComm*, 2011, **13**, 6431; (*e*) H.-C. Chen, H.-L. Hu, Z. K. Chan, C. W. Yeh, H.-W. Jia, C.-P. Wu, J.-D. Chen and J.-C. Wang, *Cryst. Growth Des.*, 2007, **7**, 698; (*f*) J.-P. Lang, Q.-F. Xu, R.-X. Yuan and B. F. Abrahams, *Angew. Chem., Int. Ed.*, 2004, **43**, 4741.

8. (*a*) M. T. Rispens, A. Meetsma, R. Rittberger, C. J. Brabec, N. S. Sariciftci and J. C. Hummelen, *Chem. Commun.*, 2003, 2116; (*b*) D. Sun, D.-F. Wang, N. Zhang, F.-J. Liu, H.-J. Hao, R.-B. Huang and L.-S. Zheng, *Dalton Trans.*, 2011, **40**, 5677; (*c*) Y. Chen, H. X. Li, D. Liu, L.-L. Liu, N.-Y. Li, H.-Y. Ye, Y. Zhang and J.-P. Lang, *Cryst. Growth Des.*, 2008, **8**, 3810; (*d*) M.-L. Tong, S.-L. Zheng and X.-M. Chen, *Chem.–Eur. J.*, 2000, **6**, 3729.

9. (*a*) B. L. Chen, N. W. Ockwig, F. R. Fronczek, D. S. Contreras and O. M. Yaghi, *Inorg. Chem.*, 2005, **44**, 181; (*b*) S. Yang, X. Lin, A. J. Blake, K. M. Thomas, P. Hubberstey, N. R. Champness and M. Schröder, *Chem. Commun.*, 2008, 6108; (*c*) H. S. Choi and M. P. Suh, *Angew. Chem., Int. Ed.*, 2009, **48**, 6865; (*d*) I. A. Ibarra, S. Yang, X. Lin, A. J. Blake, P. J. Rizkallah, H. Nowell, D. R. Allan, N. R. Champness, P. Hubberstey and M. Schröder, *Chem. Commun.*, 2011, **47**, 8304; (*e*) Q. Lin, T. Wu, S. T. Zheng, X. Bu and P. Feng,

Chem. Commun., 2011, **47**, 11852; (*f*) J. J. Wang, P. X. Gao, L. J. Gao, F. Fu, M. L. Zhang, Y. X. Ren and X. Y. Hou, *Chin. J. Struct. Chem.*, 2011, **30**, 1787.

10 (*a*) B. L. Chen, N. W. Ockwig, A. R. Millward, D. S. Contreras and O. M. Yaghi, *Angew. Chem., Int. Ed.*, 2005, **44**, 4745; (*b*) Y. Q. Lan, X. L. Wang, S. L. Li, Z. M. Su, K. Z. Shao and E. B. Wang, *Chem. Commun.*, 2007, 4863; (*c*) Z. Su, J. Fan, T. Okamura, W. Y. Sun and N. Ueyama, *Cryst. Growth Des.*, 2010, **10**, 3515; (*d*) D. S. Li, Y. P. Wu, P. Zhang, M. Du, J. Zhao, C. P. Li and Y. U. Wang, *Cryst. Growth Des.*, 2010, **10**, 2037; (*e*) M. Du, C. P. Li, C. S. Liu and S. M. Fang, *Coord. Chem. Rev.*, 2013, **257**, 1282.

11 (*a*) H. Y. He, J. M. Dou, D. C. Li, H. Q. Ma and D. F. Sun, *CrystEngComm*, 2011, **13**, 1509; (*b*) B. H. Ye, M. L. Tong and X. M. Chen, *Coord. Chem. Rev.*, 2005, **249**, 545; (*c*) F. N. Dai, H. Y. He, X. L. Zhao, Y. X. Ke, G. Q. Zhang and D. F. Sun, *CrystEngComm*, 2010, **12**, 337.

12 *Bruker, SMART, SAINT and SADABS*, Bruker AXS Inc., Madison, Wisconsin, USA, 1998.

13 G. M. Sheldrick, *SHELXS-97, Program for X-ray Crystal Structure Determination*, University of Gottingen, Germany, 1997.

14 G. M. Sheldrick, *SHELXL-97, Program for X-ray Crystal Structure Refinement*, University of Gottingen, Germany, 1997.

15 A. L. Spek, *PLATON, A Multipurpose Crystallographic Tool*, Utrecht University, Utrecht, The Netherlands, 2002.

16 M. J. Plater, M. R. St. J. Foreman, R. A. Howie, J. M. S. Skakle, S. A. McWilliam, E. Coronado and C. J. Gomez-Garcıa, *Polyhedron*, 2001, **20**, 2293.

17 X. F. Li, Y. An and Y. S. Yin, *Acta Crystallogr., Sect. E: Struct. Rep. Online*, 2007, **63**, m3117.

18 (*a*) H. Y. He, D. Collins, F. N. Dai, X. L. Zhao, G. Q. Zhang, H. Q. Ma and D. F. Sun, *Cryst. Growth Des.*, 2010, **10**, 895; (*b*) X. Zhuo, X. W. Wei, C. L. Guo, Y. Z. Li and H. G. Zheng, *Chin. J. Inorg. Chem.*, 2007, **23**, 1029; (*c*) R. K. Feller and A. K. Cheetham, *Dalton Trans.*, 2008, 2034.

19 (*a*) J. S. Hu, X. Q. Yao, M. D. Zhang, L. Qin, Y. Z. Li, Z. J. Guo, H. G. Zheng and Z. L. Xue, *Cryst. Growth Des.*, 2012, **12**, 3426; (*b*) Y. F. Cui, P. P. Sun, Q. Chen, B. L. Li and H. Y. Li, *CrystEngComm*, 2012, **14**, 4161; (*c*) F. Luo, M. S. Wang, M. B. Luo, G. M. Sun, Y. M. Song, P. X. Li and G. C. Guo, *Chem. Commun.*, 2012, **48**, 5989; (*d*) D. Liu, H. X. Li, L. L. Liu, H. M. Wang, N. Y. Li, Z. G. Ren and J. P. Lang, *CrystEngComm*, 2010, **12**, 3708; (*e*) D. S. Zhou, F. K. Wang, S. Y. Yang, Z. X. Xie and R. B. Huang, *CrystEngComm*, 2009, **11**, 2548; (*f*) J. Hunger, H. Krautscheid and J. Sieler, *Cryst. Growth Des.*, 2009, **9**, 4613; (*g*) R. K. Feller and A. K. Cheetham, *CrystEngComm*, 2009, **11**, 980; (*h*) J. S. Hu, L. F. Huang, X. Q. Yao, L. Qin, Y. Z. Li, Z. J. Guo, H. G. Zheng and Z.L. Xue, *Inorg. Chem.*, 2011, **50**, 2404.

20 H. P. Xiao, *Acta Crystallogr., Sect. E: Struct. Rep. Online*, 2006, **62**, m734.

21 K. Nakamoto, *Infrared and Raman Spectra of Inorganic and Coordination Compounds*, John Wiley & Sons, New York, 1986.

22 (*a*) D. Sun, Z.-H. Yan, M. Liu, H. Xie, S. Yuan, H. Lu, S. Feng and D. F. Sun, *Cryst. Growth Des.*, 2012, **12**, 290; (*b*) D. Sun, H.-R. Xu, C.-F. Yang, Z.-H. Wei, N. Zhang, R.-B. Huang and L.-S. Zheng, *Cryst. Growth Des.*, 2010, **10**, 4642; (*c*) S. J. Wang, S.-S. Xiong, Z. Y. Wang and J. F. Du, *Chem.–Eur. J.*, 2011, **17**, 8630.

23 (*a*) D. Sun, Z.-H. Yan, V. A. Blatov, L. Wang and D. F. Sun, *Cryst. Growth Des.*, 2013, **13**, 1277; (*b*) J. Guo, D. Sun, L. L. Zhang, Q. Yang, X. L. Zhao and D. F. Sun, *Cryst. Growth Des.*, 2012, **12**, 5649.

24 (*a*) S. Q. Zhang, F. L. Jiang, M. Y. Wu, J. Ma, Y. Bu and M. C. Hong, *Cryst. Growth Des.*, 2012, **12**, 1452; (*b*) X. T. Wu, Q. L. Zhu, T. L. Sheng, R. B. Fu, S. M. Hu, L. Chen, C. J. Shen and X. Ma, *Chem.–Eur. J.*, 2011, **17**, 3358; (*c*) S.-L. Zheng and X.-M. Chen, *Aust. J. Chem.*, 2004, **57**, 703; (*d*) M. D. Allendorf, C. A. Bauer, R. K. Bhaktaa and R. J. T. Houka, *Chem. Soc. Rev.*, 2009, **38**, 1330.

25 (*a*) Q.-L. Zhu, C.-J. Shen, C.-H. Tan, T.-L. Sheng, S.-M. Hua and X.-T. Wu, *Chem. Commun.*, 2012, **48**, 531; (*b*) Y.-J. Cui, Y.-F. Yue, G.-D. Qian and B.-L. Chen, *Chem. Rev.*, 2012, **112**, 1126; (*c*) L. L. Zhang, F. L. Liu, Y. Guo, X. P. Wang, J. Guo, Y. H. Wei, Z. Chen and D. F. Sun, *Cryst. Growth Des.*, 2012, **12**, 6215.